HAL open science

Realistic Braking Operation Simulation of Ventilated Disk Brakes

A. Floquet, Marie-Christine Baietto

▶ To cite this version:

A. Floquet, Marie-Christine Baietto. Realistic Braking Operation Simulation of Ventilated Disk Brakes. Journal of Tribology, 1996, 118 (3), pp.466-472. 10.1115/1.2831559 . hal-01951923

HAL Id: hal-01951923

https://hal.science/hal-01951923v1

Submitted on 6 Jul 2021

HAL is a multi-disciplinary open access archive for the deposit and dissemination of scientific research documents, whether they are published or not. The documents may come from teaching and research institutions in France or abroad, or from public or private research centers.

L'archive ouverte pluridisciplinaire **HAL**, est destinée au dépôt et à la diffusion de documents scientifiques de niveau recherche, publiés ou non, émanant des établissements d'enseignement et de recherche français ou étrangers, des laboratoires publics ou privés.

Distributed under a Creative Commons Attribution 4.0 International License

Realistic Braking Operation Simulation of Ventilated Disk Brakes

A. Floquet
Universite C. Bernard, Lyon I,
43 Bvd. du 11 Novembre,
69622 Villeurbanne Cédex, France

M.-C. Dubourg
I.N.S.A Laboratoire de Mécanique des Contacts,
URA CNRS 856, 20, Av. A. Einstein,
69621 Villeurbanne Cédex, France

A three-dimensional numerical method for the prediction of transient temperatures reached during realistic braking operations in a ventilated disk brake assembly is presented in this paper. This Layered FFT-FEM numerical method (Fast Fourier Transform-Finite Element Method) takes advantage of the high Peclet number "skin effect" to decouple the moving boundary contact problem from the spatially periodic but non-axisymmetric cooling associated with the vents. The first problem is modeled according to the FFT-FEM method developed previously by the authors. This technique succeeded in using high Peclet numbers for axisymmetric moving solids submitted to general loading conditions. No numerical convergence problems are encountered and short computer time is required. The second problem is modeled according to traditional three-dimensional finite element techniques. The Layered FFT-FEM results are compared with analytical results. A braking operation is simulated for an industrial ventilated disk brake.

I Introduction

Different phenomena limit the life of disk brakes: temperature rise modifies the thermal and mechanical characteristics of materials, thermomechanical distortions (Lee and Barber, 1993) give rise to instabilities and loss of efficiency and thermal crazing limits the lifetime. The complete simulation of a disk brake system requires the determination of:

1: the temperature field at every point of the component as a function of time,
2: the corresponding thermal and mechanical stresses,
3: the stress intensity factors (SIFs) at crack tips,
4: the crack growth prediction.

Such an overall project has never been undertaken for different reasons. High Peclet numbers such as those encountered in disk brakes cause numerical convergence problems in traditional finite element thermal simulations. Very fine meshes both in time and space are required to overcome these numerical instabilities (Kennedy et al., 1984) but involve very extensive computer times. The loading conditions are not axisymmetric, but for economic reasons, classical thermomechanical analyses are limited to a meridian plane. A false axisymmetric hat shaped distortion of the disk (Floquet, 1989) is obtained. Prediction of crack behaviour (crack path, crack growth rate, etc) cannot be formulated on such a basis. A new method, called FFT-FEM, was presented in a previous paper (Floquet and Dubourg, 1994) dealing with 3-D axisymmetric moving solids subjected to a transient thermal load with variable heat flux, speed, convection, etc. Furthermore, the material characteristics are temperature dependent. This hybrid method combines Fast Fourier Transform techniques (FFT) with Finite Element methods (FEM). The prediction of the transient temperatures reached during realistic braking operations is simulated for short computer time. Therefore the 2-D thermomechanical modelling limitation is now removed. Here this FFT-FEM model is extended to determine the temperature field in a ventilated disk brake assembly which geometry is spatially periodic but non-axisymmetric.

II Ventilated Moving Solid Under Nonaxisymmetric Transient Heat Conditions: The Thermal Analysis

II.1 Brief Description of the FFT-FEM Technique. An original method for the analysis of three dimensional axisymmetric moving solids submitted to nonaxisymmetric transient heat conditions was presented in a previous paper by Floquet and Dubourg. This FFT-FEM method combines Fourier Integral Transform techniques and finite element methods. The method is based on Fourier Transform with respect to the space variable θ corresponding to the disk sliding speed direction. In practice, this is done by the Fast Fourier Transform (FFT) technique (Brigham, 1974). This FFT technique is combined with the Singleton method (Singleton, 1969).

Any axisymmetric geometry can be considered. The heat-conduction equation considered in the cylindrical coordinates system (r, θ, z) attached to a fixed reference axis is (cf. Fig. 1):

$$\frac{\partial^2 T}{\partial r^2} + \frac{1}{r}\frac{\partial T}{\partial r} + \frac{\partial^2 T}{\partial z^2} + \frac{1}{r^2}\frac{\partial^2 T}{\partial \theta^2} = \frac{1}{D}\left(\frac{\partial T}{\partial t} + \omega \frac{\partial T}{\partial \theta}\right)$$

$$\begin{cases} \text{Boundary Condition (BC)} \ : \ T(r, \theta, z, t) = T_c(r, \theta, z, t) \quad \text{on} \quad (S_1) \\ k\,\overrightarrow{\text{grad}}\, T \cdot \vec{n} = q_c(r, \theta, z, t) \quad \text{on} \quad (S_2) \\ -k\,\overrightarrow{\text{grad}}\, T \cdot \vec{n} = h(T - T_a) \quad \text{on} \quad (S_3) \\ \text{Initial Condition (IC)} \ : \ T(r, \theta, z, t = 0) = T_i(r, \theta, z) \end{cases} \tag{1}$$

where

D is the material thermal diffusivity and h is the heat-transfer coefficient at the surface of solid which takes into account convection and radiation. Ta is the environment temperature, S1, S2, and S3 are arbitrary surfaces on which temperature, heat-flux or convection are imposed.

The application of a transform integral to (1) has the effect of reducing the dimensionality of the problem. The space variable considered, θ here, is transformed into a discrete parameter, the frequency f, and partial derivatives with respect to θ are removed from the heat-conduction equation. The domain (V) and the bounded surfaces are respectively transformed into the meridian plane Ω, $\Gamma 1$, $\Gamma 2$ and $\Gamma 3$. The transformed equation has to be solved on the meridian plane Ω.

The Fourier Integral Transform with respect to the θ variable for a cyclic function $g(x)$ with a period of $2L$, is defined by $\bar{g}(f)$

$$\bar{g}(f) = \int_0^L g(x) \exp(-2j\pi f x)dx \tag{2}$$

with $f = n/L$, $n \in N$, j is a pure imaginary number.

The inverse transform is done by Fast Fourier Transform algorithm (Brigham, 1974, Singleton, 1969).

The integral transformation of the system (1) by the application of the transform (2) yields

$$\begin{cases} \dfrac{\partial^2 \bar{T}}{\partial r^2} + \dfrac{1}{r}\dfrac{\partial \bar{T}}{\partial r} + \dfrac{\partial^2 \bar{T}}{\partial z^2} - \left(\dfrac{\alpha^2}{r^2} + j\dfrac{\beta}{D}\right)\bar{T} = \dfrac{1}{D}\dfrac{\partial \bar{T}}{\partial t} \quad \text{on} \quad (\Omega) \\ \text{BC} \ : \ \bar{T}(r, z, t) = \bar{T}_c(r, z, t) \quad \text{on} \quad (\Gamma_1) \\ k\,\overrightarrow{\text{grad}}\, \bar{T}.\vec{n} = \bar{q}_c(r, z, t) \quad \text{on} \quad (\Gamma_2) \\ -k\,\overrightarrow{\text{grad}}\, \bar{T}.\vec{n} = h(\bar{T} - \bar{T}_a) \quad \text{on} \quad (\Gamma_3) \\ \text{IC} \ : \ \bar{T}(r, z, t = 0) = \bar{T}_i(r, z, 0) \quad \text{on} \quad (\Gamma) \end{cases} \tag{3}$$

with

$$\alpha = 2\pi f$$

$$\beta = 2\pi f \omega$$

$$f = n/2\pi$$

The speed effect is no longer associated with the temperature derivative with respect to θ, but with the function itself. Furthermore the oscillations associated with high Peclet numbers are removed. The finite element technique is applied directly. The weak formulation of the problem is given by:

$$-\int_\Omega \overrightarrow{\text{grad}}\, \bar{T} \cdot \overrightarrow{\text{grad}}\, W d\Omega + \int_\Omega \frac{1}{r}\frac{\partial \bar{T}}{\partial r} W d\Omega - \alpha^2 \int_\Omega \frac{\bar{T}}{r^2} W d\Omega$$
$$-j\beta \int_n \frac{\bar{T}W}{D} d\Omega + \int_{\Gamma_2} \frac{\bar{q}_c}{k} W d\Gamma - \int_{\Gamma_3} \frac{h}{k}(\bar{T} - \bar{T}_a) W d\Gamma \tag{4}$$
$$= \int_\Omega \frac{1}{D}\frac{\partial T}{\partial t} d\Omega$$

with:

$$\bar{T}(r, z, t) = \bar{T}_c(r, z, t) \quad \text{on} \quad \Gamma_1$$
$$\bar{T}(r, z, t = 0) = \bar{T}_i(r, z, 0) \quad \text{on} \quad \Omega$$

D is a linear piecewise function of the temperature. h is a bilinear piecewise function of temperature and speed. Their values over a finite element are constant during a time step and are determined according to the average value at the previous time step of the temperature for D and to the average values of the temperature and speed for h.

The transformed quantities are complex variables with real and imaginary parts. The transformed system (4) is solved using two-dimensional finite elements with two degrees of freedom per node (real and imaginary parts). It finally leads to a differential equation system solved here by an explicit Euler classical method.

The FFT-FEM results were compared with analytical results and the comparison showed an excellent agreement (Floquet et Dubourg, 1994, Floquet, 1985). Furthermore, the efficiency of the method was demonstrated in a 3-D simulation problem: the temperature distribution in a disk brake assembly was predicted during a realistic braking operation.

II.2 The Layered FFT-FEM Technique. The axisymmetrical property no longer holds for ventilated disk brakes. A correct model requires consideration of a mobile reference axis, linked to the disk. The initial problems related to the existence of numerical instabilities when the Peclet number is greater than 2 arise again. In this paper, the Layered FFT-FEM method, based on the pioneering FFT-FEM method, is proposed to predict the temperature distribution in spatially periodic but nonaxisymmetric moving solids.

High Peclet numbers in practical systems and particularly in brake systems induce surface heating in a thin layer adjacent to the surface (Archard, 1958, Colin et al., 1988), points at greater depth responding to the time-average heat input only (Floquet, 1985). The new model rests on this basic result.

The complete system is therefore divided into different parts. Each part is analyzed either with the FFT-FEM method or with the 3-D finite element technique (3-D FEM), according to geometrical and boundary conditions. The ventilated disk brake system is divided into (cf. Fig. 2):

the mobile part of the brake, composed of the disk itself and the rim:

- the parts adjacent to both heated surfaces are modeled according to the FFT-FEM technique: these regions correspond to hub caps. The axisymmetrical property is verified, high Peclet numbers are encountered,
- the central part corresponding to the vents is analyzed with the 3-D FEM technique in a reference axis linked to the disk. The temperature distribution is independent of θ at this depth.

a fixed part, made of the pads and caliper, modeled with the 3-D FEM technique.

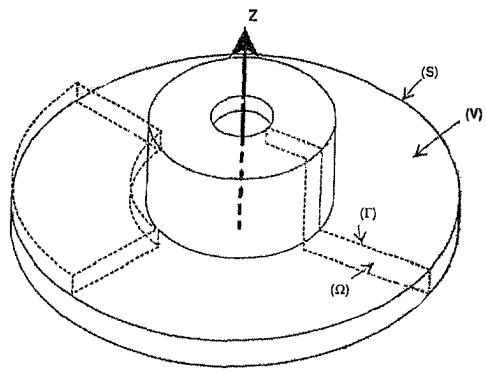

Fig. 1 Axisymmetric disk brake assembly. Meridian plane (z, r)

In practice, the thickness of the central part is greater than the effective vent diameter in order to enhance the heat exchange. The matching point between the FFT-FEM and 3-D FEM regions is located at a much greater depth than the depth of the thin heating layer corresponding to the speed effect. Thus it is not necessary to recreate a finite element mesh at each time step for each Peclet number. This matching point can be assumed to be axisymmetric, as the temperature field and the temperature gradients are practically independent of θ at this depth leading to axisymmetric boundary conditions. Further, the cooling phenomenon associated with the vents schematically corresponds to a pulsed cooling flux at a frequency $f = nc*\omega$, where nc is the number of vents and ω the rotational speed. According to Carslaw and Jaeger (1959) the temperature variations along θ decrease as $\alpha e^{-\alpha z}$ where z is the depth from the surface of the vent. It is a correct assumption to consider that the temperature field is uniform along θ in the central part one millimeter from the vent. Consequently significant improvements in the 3-D FEM modeling leading to a decrease in computer time are performed by taking advantage of these axisymmetric boundary conditions and of the spatially periodic geometry of the vents. Only a portion of the central part corresponding to one vent is analyzed with the finite element technique. The period may also correspond to several vents if part of them are linked to the upper hub cap, and the other ones to the lower hub cap. These simplifications do not constitute a limitation of the model. Variations regarding θ can be handled and will lead to only a very small difference in the temperature field $T(r, \theta, z, t)$, but to longer computing times.

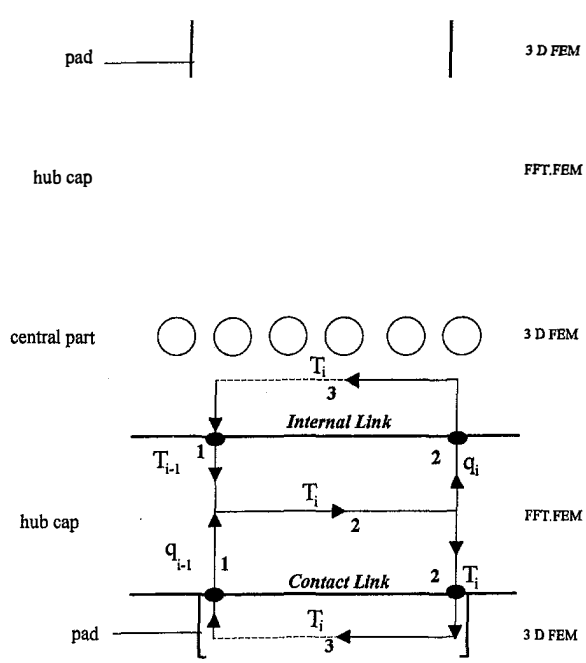

Fig. 2 Schematic partition of a ventilated disk brake assembly into 5 regions depending on the use of FFT-FEM or 3-D FEM techniques. Heat transfer methodologies from FFT-FEM to 3-D FEM regions (internal link) and 3-D FEM to FFT-FEM regions (contact link). ● indicates boundary conditions between regions. → indicates the direction of the loop. 1, 2, 3 are the stages of the loop. – – – indicates change of time step.

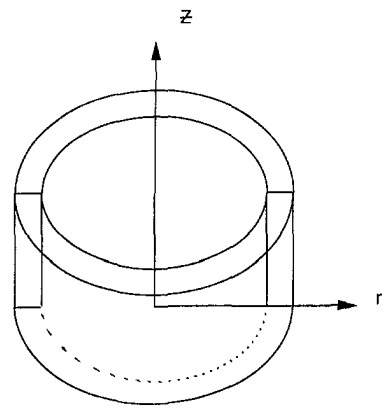

Fig. 3(a) Axisymmetric ring geometry

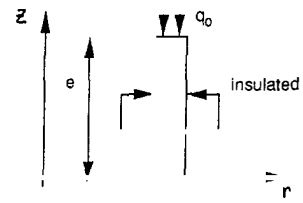

Fig. 3(*b*) Meridian plane ring and loading conditions

The temperature field determination requires therefore to partition the disk brake assembly into five regions where either the FFT-FEM or 3-D FEM method is used. Thus boundary conditions at the interface between two regions are necessary for the heat transfer from an FFT-FEM to a 3-D FEM region and viceversa. Two kinds of connection hold (cf. Fig. 2):

the connection between hub caps and the central part, called the internal link,

the connection between the hub caps and the pads, called the contact link.

Initially a uniform temperature field holds in the disk brake assembly. During a time step, the FFT-FEM problem in hub caps is solved first, then the 3-D FEM ones in the central part and the pads. Concerning the temperature field determination in both hub caps, the boundary conditions considered are prescribed heat flux at interfaces between pad and hub cap and prescribed temperature at interfaces between hub caps and the central part. At the first time step, the braking energy is assumed to dissipate totally in the hub caps and the imposed temperature is equal to the environment temperature. At a time step i, the braking energy is naturally partitioned between pads and hub caps depending on the temperature field in pads and hub caps and the imposed temperature is equal to the temperature determined at the time step $i - 1$ in the central part.

The temperature field is thus determined in both hub caps (stage 2 of the internal link). The temperature gradients are calculated at interfaces between hub caps and the central part (still stage 2 of the internal link), and imposed as boundary conditions for the temperature field determination in the central part according to 3-D FEM method (Stage 3 of the internal

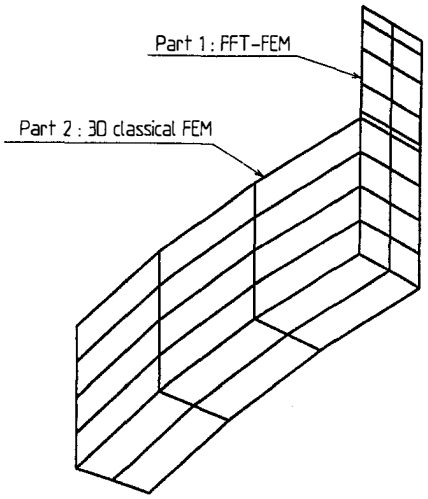

Fig. 4(a) Ring partition into FFT-FEM and 3D FEM regions

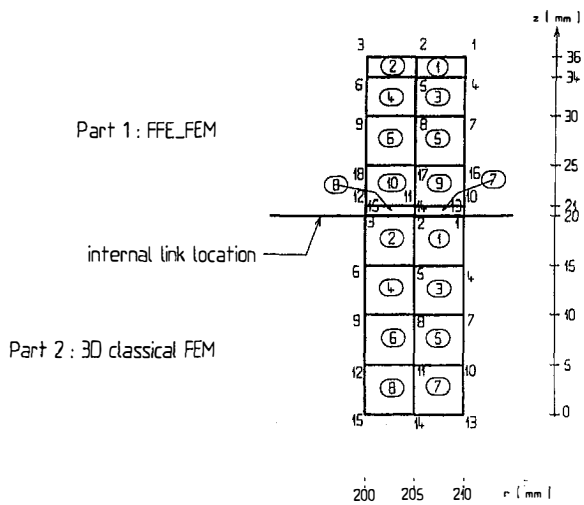

Fig. 4(*b*) FFT-FEM and 3D FEM meshes of the meridian plane. Internal link location

Fig. 4 Layered FFT-FEM mesh of the ring

link). If only a portion of the central part is analyzed, the heat flux considered corresponds to a fraction of the total outgoing heat flux from the FFT-FEM problem. At the same time the temperatures at interfaces between hub cap and pad (stage 2 of

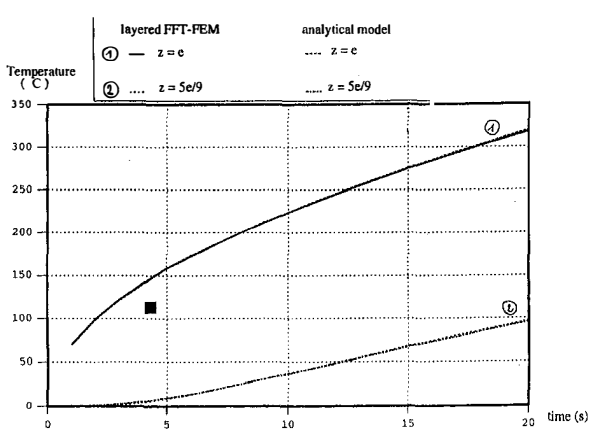

Fig. 5 Temperature field versus time at z = e and z = 5e/9 according to layered FFT-FEM and analytical models

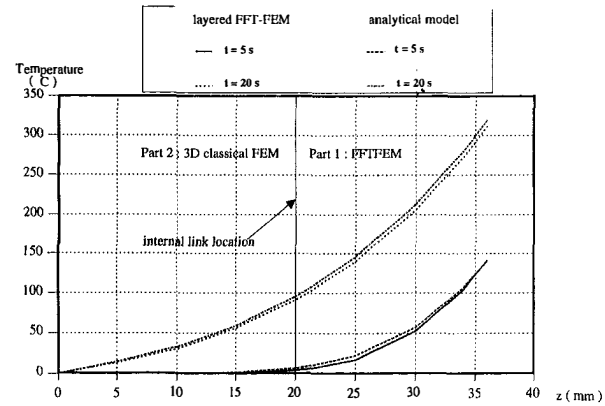

Fig. 6 Temperature field versus z at t = 5 s and t = 20 s according to layered FFT-FEM and analytical models

the internal link) are imposed as boundary conditions for the temperature determination in the pads according to 3-D FEM method (Stage 3 of the contact link). Temperature gradients are then computed at boundaries between pad and hub cap and will be used to determine the boundary conditions in term of heat flux for time step $i + 1$ as the heat flux entering the hub caps at time step $i + 1$ is equal to the total frictional heat flux minus the heat flux entering the pads at time step i. The time offset considered here leads to very minor errors. This heat flux will be imposed as boundary conditions at time step $i + 1$ for the temperature solution in the hub caps.

At time step $i + 1$, the complete procedure is performed again.

Transfer loops for the contact and internal links are oppositely organized. This is done to avoid convergence problems. Temperature variations are more important in the hub caps than in the central part. It is therefore logical to impose the hub cap temperature gradients as boundary conditions for determining the temperature field in the central part. The hub cap/pad connection cannot be performed in a similar way due to numerical instabilities. An opposite procedure is adopted. The braking energy decreased by the pad absorbed energy is imposed to the hub caps that give back a temperature field at the connection surface.

III Comparisons With Analytical Results

The validation of the FFT-FEM method was performed previously for cases with and without speed effects (Floquet and Dubourg, 1994).

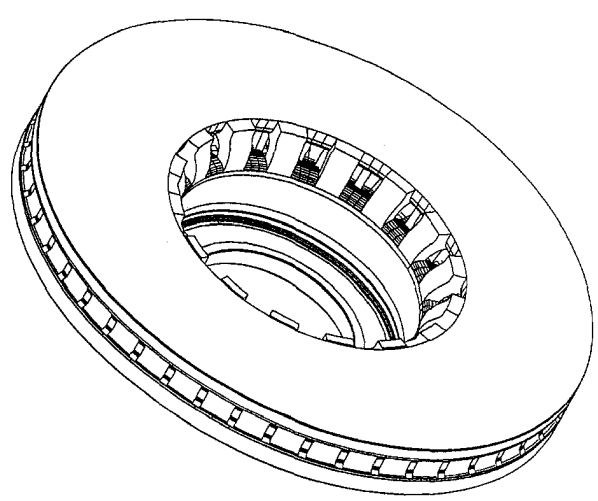

Fig. 7 Vehicle ventilated disk brake

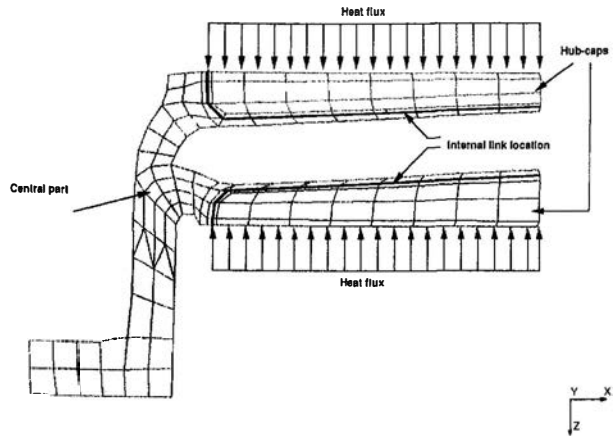

Fig. 8(*a*) Ventilated disk brake assembly: meridian plane *xOz* crosses a vent

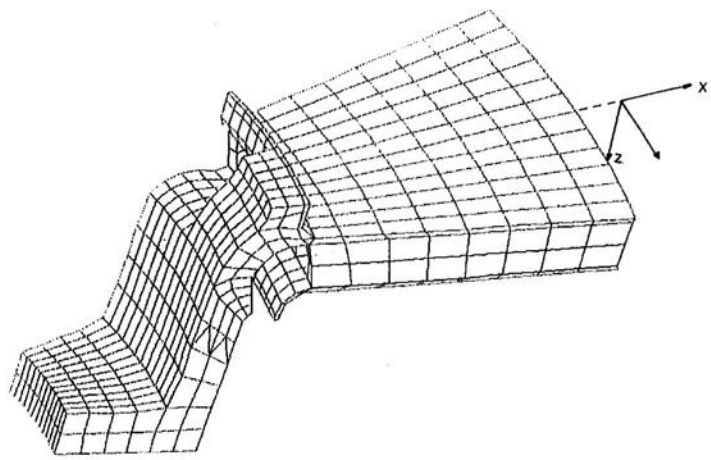

Fig. 8(*b*) 3-D FEM mesh of the central part of the ventilated disk brake assembly

The heat transfer between the FFT-FEM and 3-D FEM regions is the main point to check in the Layered FFT-FEM method. The temperature field at the matching point between the two regions is roughly independent of θ. The speed effect has there no influence on the heat transfer and will moreover smooth possible discrepancies. Thus a very simple case without speed effects is considered to compare the Layered FFT-FEM results with analytical ones and to check the heat transfer in the z direction. The attention is directed to the temperature distribution at the internal link location.

A ring is considered (cf. Fig. 3(*a*)). The meridian plane is a rectangular (cf. Figure 3(*b*)). This region is initially at zero temperature. For times t greater than 0, a zero temperature is imposed to boundary $z = 0$, a constant heat flux is applied at

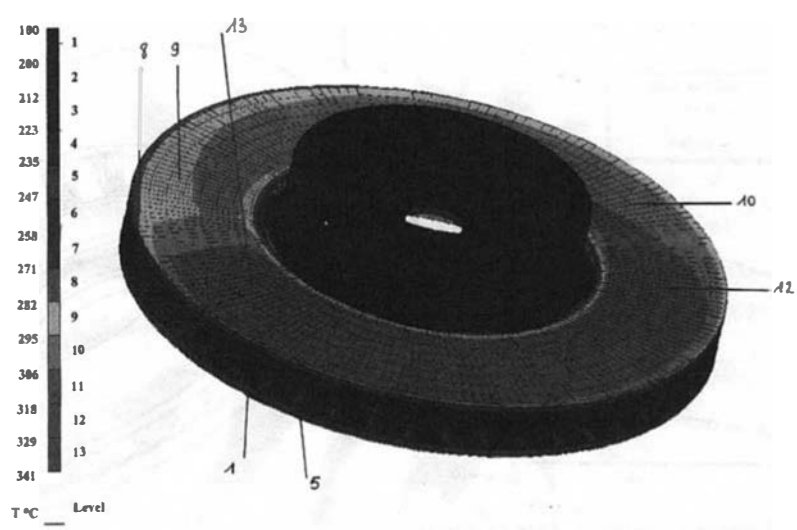

Fig. 9 Disk brake temperature map at t = 7 s

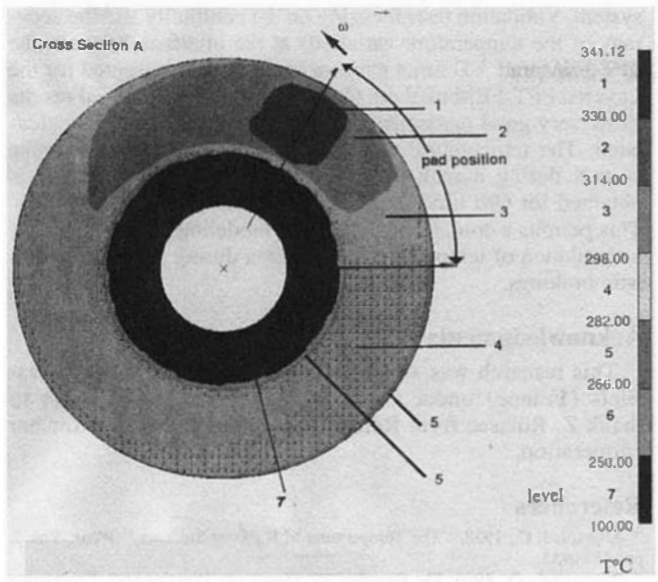

Fig. 10 Top view of the disk brake temperature map at t = 7 s

boundary $z = e$, $q = qo$, $qo = 10^6$ W/m^2. The side boundaries are insulated. Height e is equal to 0.036 m. The thermal material properties considered are $h = 100$ W/m^2 °C, $k = 50$ W/m°C, $\rho = 7800$ kg/m^3, $C = 500$ J/kg°C. The analytical solution of this problem is (Oziski, 1980).

$$T(t, \theta, z) = -\frac{q_o}{k} \sum_{m=1}^{\infty} \frac{-(1)^m}{\beta_m} [1 - \exp(-D\beta_m^2 t)] \sin \beta m z$$

with

$$\beta m = (2m - 1) \frac{\pi}{2e}$$

The meridian plane of the ring is divided into two parts (cf. Fig. 4(a)):

Part 1 is analyzed using the FFT.FEM method. Two dimensional four nodes finite elements are used. The thickness of the last layer of finite elements of the FFT-FEM grid is small in order to determine accurately the outgoing temperature gradients. Taking an identical standard thickness for these elements would lead to an overestimation of the temperature gradients and thus of the interface temperature field by roughly 10 to 20 percent. The optimum ratio between the thicknesses of the last two layers of finite elements is found to be 0.25.

Part 2 is modeled with the 3-D FEM method. Twenty four hexaedric finite elements are considered (8 in the meridian plane, 3 in the circumferential direction). As this problem is axisymmetric (geometrically and running conditions), it is not necessary to model the whole annulus.

The ring partition into FFT-FEM and 3-D FEM regions is presented Fig. 4(a). Figure 4(b) gives the FFT-FEM and 3-D FEM grids of the meridian plane. The location of the internal link ($z = 5e/9 = 20$ mm) is specified. The thickness of the last two elements of the FFT-FEM grid (numbered 7 and 8) is effectively small.

Comparisons between Layered FFT-FEM and analytical results are presented in Figs. 5 and 6. Figure 5 shows the temperature variations versus time at $z = e$ (where the heat-flux is applied) and at $z = 5e/9$ corresponding to the internal link location. Excellent agreement is obtained both at $z = e$, mostly validating the FFT-FEM technique, and at $z = 5e/9$ justifying the FFT-FEM and 3-D FEM combination. Figure 6 shows the temperature variations versus z at times $t = 5$ and 20 seconds. The Layered FFT-FEM and 3-D FEM results are in good agreement. Further no discontinuity in the Layered FFT-FEM temperature profile at the internal link location is observed. The heat transfer between the FFT-FEM and 3-D FEM regions is therefore correctly performed.

This simple test has permitted to verify the connection between FFT.FEM and the 3-D FEM methods, which was the main point to check in the Layered FFT-FEM technique. Tests were also performed on axisymmetric solids submitted to transient heat-flux conditions. The thermal analysis was performed by the FFT-FEM and by the Layered FFT-FEM techniques. Results were in good agreement.

IV Prediction of the Temperature Field During a Braking Operation in an Automotive Vehicle Ventilated Disk Brake

An industrial ventilated disk brake is presented in Fig. 7. the braking operation lasts 7.5 seconds, the speed decreases linearly from 105 km/h (56/s) to 70 km/h (37, 1/s) and the energy dissipated is 1200 kJ. The heat flux is assumed to be constant over the pads. More realistic contact conditions between pads and disk and consequently heat input distribution will be taken into account in the future. The initial temperature field is constant and equal to 120°C. The boundary conditions are the following:

environment temperature 50°C,
imposed temperature in the region close to the rim 100°C,
different convection conditions: on hub cap tracks, vents and elsewhere,
pads correspond to a 60° degree arc length sector,

The thermal properties are temperature related. They are basically those of a classical cast iron.

The disk brake is divided into three parts, two hub caps and a central part. Figure 8(a) shows meridian plane xOz. This plane crosses a vent. The central part and both hub caps are meshed. The internal link locations and also the heat-flux distribution are indicated. Each hub cap is modeled with 35 quadrangle elements with two degrees of freedom resulting in 48 nodes. 192 frequencies are considered but only 30 are used for the calculation. The 3-D mesh of the central part is presented in figure 8b. A 22.5 degree angular sector only is modeled containing six vents: 3 are attached to the upper hub cap and the three others to the lower hub cap. This particular design even increases the heat energy dissipation and leads to symmetrical temperature distribution between the hub caps. This portion of the central part is described with 948 three-dimensional elements (both hexaedric and prismatic) with one degree of freedom leading to 1533 nodes. The Layered FFT-FEM method requires there-

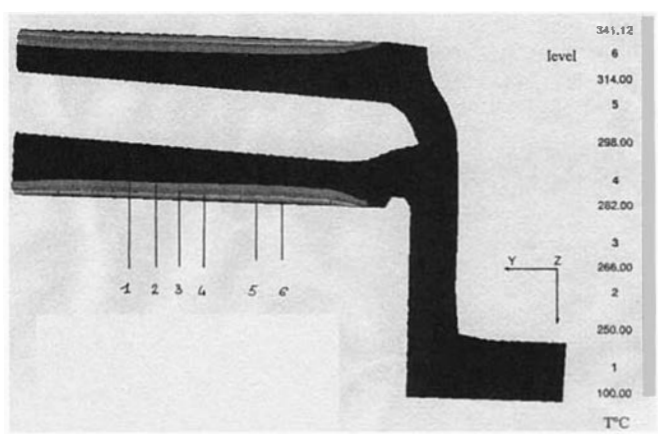

Fig. 11 Temperature map in the meridian plane corresponding to cross section A at t = 7 s

fore the solution of 60 (2*30 frequencies) two-dimensional problems with 96 (48*2) degrees of freedom for both hub caps and the central part three-dimensional problem with 1533 degrees of freedom for one time step. This Layered FFT-FEM grid correspond to classical 3-D finite element mesh of 28608 elements and 34560 nodes, divided into 13440 elements for both hub caps (192 frequencies*35 elements*2 hub caps) and 15168 elements (948 elements*16 angular sectors) for the central part!

The braking operation is studied during 30 seconds corresponding to 600 time steps. The temperature contours at t equals 7 seconds are presented in Figs. 9, 10, and 11. The disk brake temperature map shown in Figure 9 highlights different points: the temperature is a function of θ, its maximum is localised at the surface over the pad domain, the temperature variations around each vent clearly identify its location. Figure 10 is a top view of the disk brake temperature distribution. The maximum temperature is located at the end of the pad domain. Finally a temperature map in meridian plane corresponding to cross section A indicated in Fig. 10 is presented in Fig. 11. The temperature decreases through the thickness of the hub caps, from the upper surface where the heat-flux is applied to the interface with the central part. A slight dissymmetry in the temperature field is observed. This is due to a difference in the heat-flux distribution over the hub caps.

This transient thermal simulation takes 20 CPU minutes on a Digital Alpha 400 (2 seconds per time step). The classical 3-D finite element elastic calculation of the same geometry configuration (34560 nodes and 103680 degrees of freedom) takes 100 CPU minutes for one time step.

Conclusion

The Layered FFT-FEM method is presented here to deal with geometrically periodic but nonaxisymmetric moving solids such as ventilated disk brakes. This method is based on a partition of the system between moving axisymmetrical parts (hub caps) and repetitive non axisymmetric part (vents). The former part is analyzed using the FFT-FEM method and the latter one with the 3-D FEM technique. The accuracy of the FFT-FEM method was verified in previous work using an axisymmetric disk brake system. Validation tests focusing on the continuity and the accuracy of the temperature variations at the interface between the FFT-FEM and 3-D finite element methods are presented for the Layered FFT-FEM method. Comparisons with analytical results show very good agreement. Finally an industrial case is calculated. The temperature distribution in a ventilated disk brake system during a realistic braking operation (30 seconds) is obtained for 600 time steps. It requires only 20 CPU minutes. This permits a complete 3-D thermal modeling and in particular a simulation of temperature progression during successive realistic brakings.

Acknowledgments

This research was supported by Renault Véhicules Industriels (France) under Grant N°2252. The authors wish to thank Z. Roissac from Renault Véhicules Industriels for her cooperation.

References

Archard, J. C., 1958, "The Temperature of Rubbing Surfaces," *Wear*, Vol. 2, pp. 438–455.

Brigham, E. O., 1974, *The Fast Fourier Transform*, Prentice Hall, Englewood Cliffs, NJ.

Carslaw, H. S., Jaeger, J. C., 1959, *Conduction of Heat in Solids*, Oxford, Clarendon Press.

Colin, F., Floquet, A., and Play, D., 1988, "Thermal Contact Simulation in 2-D and 3-D Mechanisms," ASME JOURNAL OF TRIBOLOGY, Vol. 110, No. 2, pp. 247–252.

Floquet, A., 1985, "Les températures éclairs en système multicouche," EUROTRIB, Lyon, Session DII: Moyens d'investigation nouveaux Méthodes de Calcul, Vol. I, p. 4.2.1–4.2.10.

Floquet, A., 1989, "Modélisation thermique bidimensionnelle des instabilités du freinage," Contrat Régie Renault H3-13-502, 25 pp.

Floquet, A., and Dubourg, M. C., 1994, "Nonaxisymmetric effects for three dimensional analysis of a brake," ASME JOURNAL OF TRIBOLOGY, Vol. 116, pp. 401–408.

Kennedy, F. E., Colin, F., Floquet, A., and Glovsky, R., 1984, "Improved techniques for finite element analysis of sliding surface temperatures. Numerical and experimental methods applied to Tribology," D. Dowson, C. M. Taylor, M. Godet, and D. Berthe, eds., Butterworths, Westbury House, pp. 138–150.

Lee, K., and Barber, J. R., 1993, "Frictionally-Exited Thermoelastic Instability in Automotive Disk Brakes," ASME JOURNAL OF TRIBOLOGY, Vol. 115, pp. 607–614.

Ozisik, N. M., 1980, *Heat Conduction*, Wiley, New York, p. 687.

Singleton, P. C., 1969, "An Algorithm for Computing the Mixed Radix Fast Fourier Transform," *IEEE Transaction on Audio and Electroacoustics*, Vol. 17, No. 2, pp. 93–103.